Electronic Supplementary Material (ESI) for Environmental Science: Nano.

Graphene oxide modulated dual S-scheme ultrathin heterojunctions with iron phthalocyanine and phase-mixed bismuth molybdate as wide visible-light catalysts

Donghui Hu[a, b], Tao Song[a], Amir Zada[c], Rui Yan[a], Zhijun Li[a], Ziqing Zhang[a], Ji Bian[a], Yang Qu[a]* and Liqiang Jing[a]*

[a] Key Laboratory of Functional Inorganic Materials Chemistry (Ministry of Education), School of Chemistry and Materials Science, International Joint Research Center for Catalytic Technology, Heilongjiang University, Harbin, 150080, P. R. China.

[b] School of Science, Heihe University, Heihe, 164300, P. R. China.

[c] Department of Chemistry, Abdul Wali Khan University Mardan, Mardan 23200, Pakistan.

*Corresponding authors Email: quyang@hlju.edu.cn (Y. Qu), jinglq@hlju.edu.cn (L. Q. Jing)

Tel/Fax numbers: +86-0451-86604760

Experimental section

Structural characterization

The X-ray powder diffraction (XRD) patterns of the samples were measured with a Bruker D8 Advance diffractometer, using CuKa radiation. Ultraviolet-Visible (UV-Vis) absorption spectra of the samples were acquired on Model Shimadzu UV-2700 spectrophotometer using $BaSO_4$ as the reference. The morphology and structure of samples were characterized by a scanning electron microscope (SEM, S-4800, Hitachi) and a transmission electron microscope (TEM, JEM-2010, JEOL). The thickness of the samples was analyzed by atomic force microscopy (AFM) on a multimode nanoscope VIII instrument (Bruker) with mica as the base. The FEI Tecnai G2 S-Twin equipped with Energy-Dispersive X-ray (EDX) detector was used to acquire elemental analyses of the samples. The Fourier-transform infrared (FT-IR) spectra were collected with a Thermo Scientific Nicolet iS50 FT-IR spectrometer, KBr as the diluents. The Raman spectra were recorded with a Renishaw inVia Confocal Raman spectrometer with a 532 nm laser as excitation source. X-ray photoelectron spectroscopy (XPS) surveys were analyzed by using a Kratos-AXIS ULTRA DLD, Aluminum (Mono) as the X-ray source.

Photocatalytic activity evaluation

The activities of the samples were evaluated by photodegradation of TC using a 150 W white-light LED light (28.3 mW/cm^2). Firstly, 0.03 g catalysts and TC solution (100 mL, 10 mg L^{-1}) were mixed in a 250 ml beaker under stirring for 30 min in dark to reach the adsorption-desorption equilibrium. Secondly, the above solution was degraded in the open beaker for 10 min under visible-light irradiation. Finally, the concentration

of TC was analyzed by the UV-Vis spectrometer (Shimadzu UV-2700).

The procedure of the TOC test was the same as that of TC photodegradation. The TOC test conditions are as follows: the temperature is 680 °C, the O_2 pressure is 200 ± 10 kPa, and each data point is the average result after three tests. During the procedure, 15 mL of the solutions were sampled at determined times during the degradation process and analyzed immediately by the TOC-L (Shimadzu) after filtration through a 0.22 mm membrane. The TOC removal was calculated using the following equation:

$$TOC\ removal\ \% = \frac{TOC_0 - TOC_t}{TOC_0} \times 100\%$$

TOC_0: the value of original TOC; TOC_t: the value of TOC at determined time.

Recycle experiment was carried out by the same procedure. For each run, the used photocatalyst was centrifuged and alternately washed with deionized water and ethanol. After that, it was dried at 80 °C for 4 h.

Hydroxyl radical measurement

The specific method for the hydroxyl radical test was as follows: 0.05 g of the catalyst was placed in 50 mL of coumarin solution at a concentration of 2×10^{-4} M. The mixture was stirred for 30 min before the experiment, to ensure that it reached the adsorption-desorption equilibrium. After irradiation for 1h under visible-light irradiation, appropriate amount of the suspension was centrifuged in a 10 mL centrifuge tube and the supernatant was transferred into a Pyrex glass cell for the fluorescence measurement of 7-hydroxycoumarin by a spectrofluorometer (Perkin-Elmer LS55).

Photoelectrochemical and electrochemical measurement

The film electrode was fabricated as follows: firstly, 10 mg of samples, 0.1 mL of Nafion and 0.9 mL of ethanol were mixed thoroughly to form a slurry. Then the slurry was coated on the FTO glass electrode (1.0 × 1.0 cm). At last, the coated electrode was dried at 60 °C for 30 min. Photoelectrochemical (PEC) and electrochemical (EC) measurements were carried out on the IVIUM V13806 electrochemical workstation with traditional three-electrode system. The as-prepared sample films were used as working electrodes in a sealed quartz cell. A platinum plate (99.9%) and saturated KCl Ag/AgCl electrode were used as the counter electrode and reference electrode, respectively. 0.2 M $NaSO_4$ solution was used as electrolyte. High-purity N_2 or O_2 (99.999%) was employed to bubble through the electrolyte to keep the saturated gas in the EC experiment. PEC experiments were performed in a quartz cell using a 300 W xenon lamp with a cut-off filter ($\lambda > 420$ nm) as the illumination source. Mott-Schottky plots were implemented at frequencies of 500, 1000, and 1500 Hz. All the experiments were performed at room temperature (about 25 ± 3 °C).

Superoxide radical measurement

$\bullet O_2^-$ species were confirmed by EPR which were carried out on a Bruker EMX plus model spectrometer operating at the X-band frequency. The reactive $\bullet O_2^-$ species were detected with the assist of DMPO as a spin trap under visible-light irradiation. The concentration of DMPO was 50 mM and $\bullet O_2^-$ were determined in methanol phase.

O_2 temperature-programmed desorption measurement

Temperature-programmed desorption (TPD) of O_2 was carried out in a conventional apparatus by Chemisorption Analyzer (Tp 5080 Chemisorb) equipped with a TCD detector. About 50 mg of catalysts were pretreated at 110 °C for 1 h under ultra-high-pure He gas flow with the rate of 30 mL/min^{-1}. The highly pure O_2 was introduced at a constant temperature of 30 °C under the flow rate of 30 mL min^{-1} for 1 h. The physically adsorbed O_2 was removed by being exposed with ultra-high-pure He at 30 °C for 1 h. Then the temperature was increased to 400 °C with the heating rate of 10 °C min^{-1} under ultra-high-pure He. Finally, the desorbed O_2 was monitored by Chemisorption Analyzer.

Intermediates measurement

The various intermediates during TC photodegradation were obtained by using a typical experiment. Adsorption-desorption equilibrium and photocatalytic degradation process were same with the above photocatalytic activity experiments. After that, a certain volume liquid was taken out for measurement at regular interval during the photocatalytic degradation process. The intermediates were detected with LC-MS/MS (liquid chromatography tandem mass spectrometry) (Xevo TQD, USA) technique. The fragments of the main reaction intermediate were analyzed through scan mode.

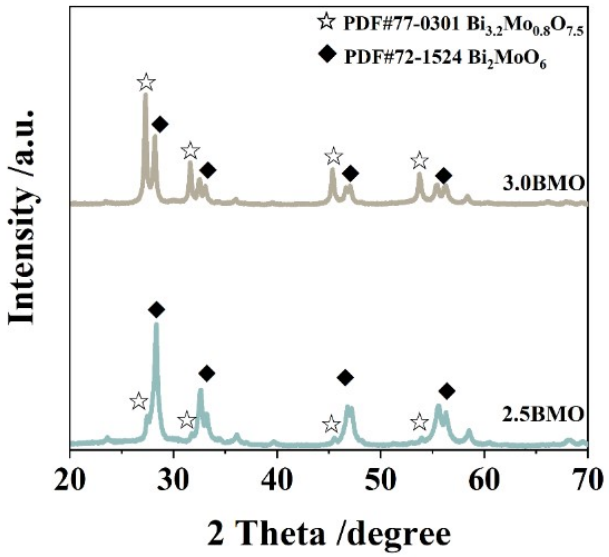

Fig. S1. XRD patterns of 2.5BMO and 3.0BMO.

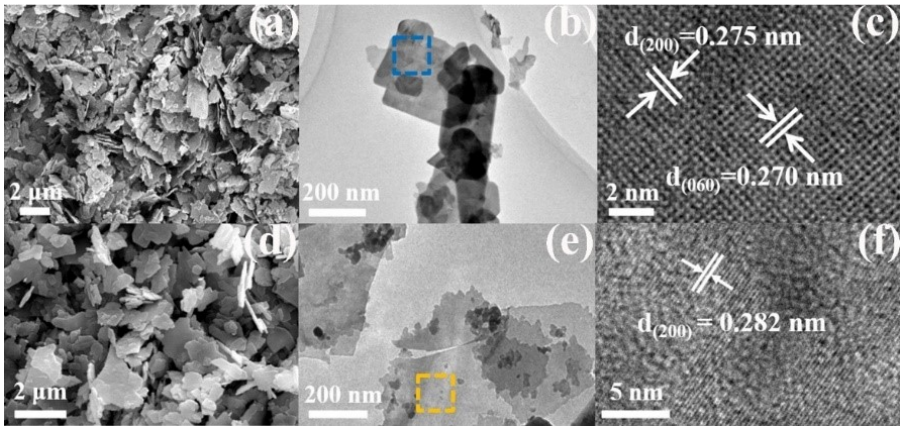

Fig. S2. SEM, TEM, and HRTEM images of 2.0BMO (a-c) and 4.0BMO (d-f).

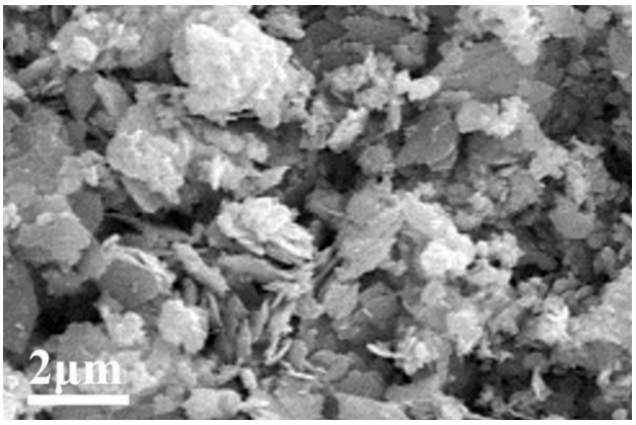

Fig. S3. SEM image of 2.7BMO.

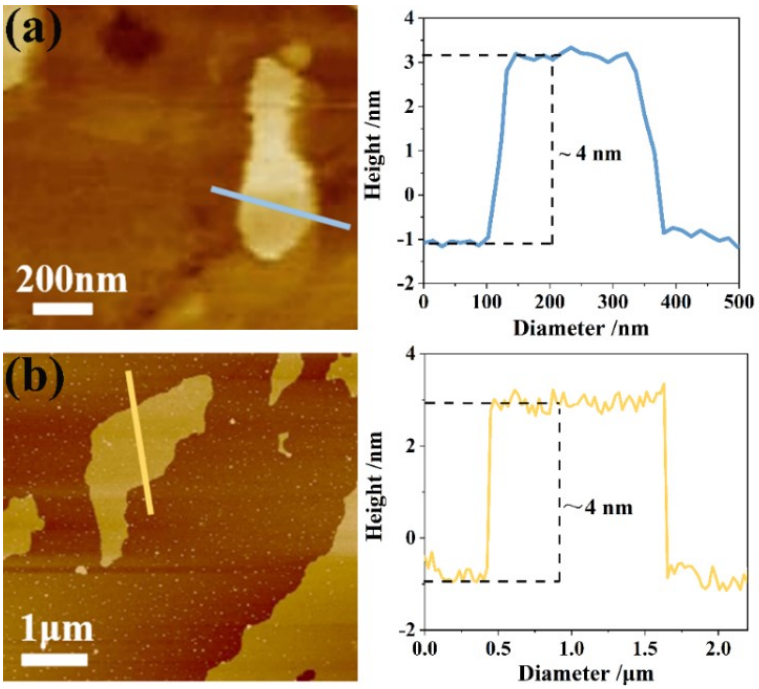

Fig. S4. AFM images and high profiles of 2.0BMO (a) and 4.0BMO (b).

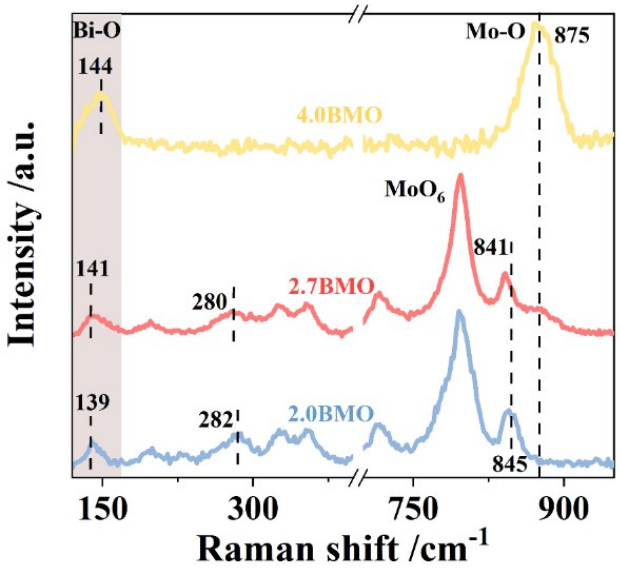

Fig. S5. Raman spectra of 2.0BMO, 4.0BMO, and 2.7BMO.

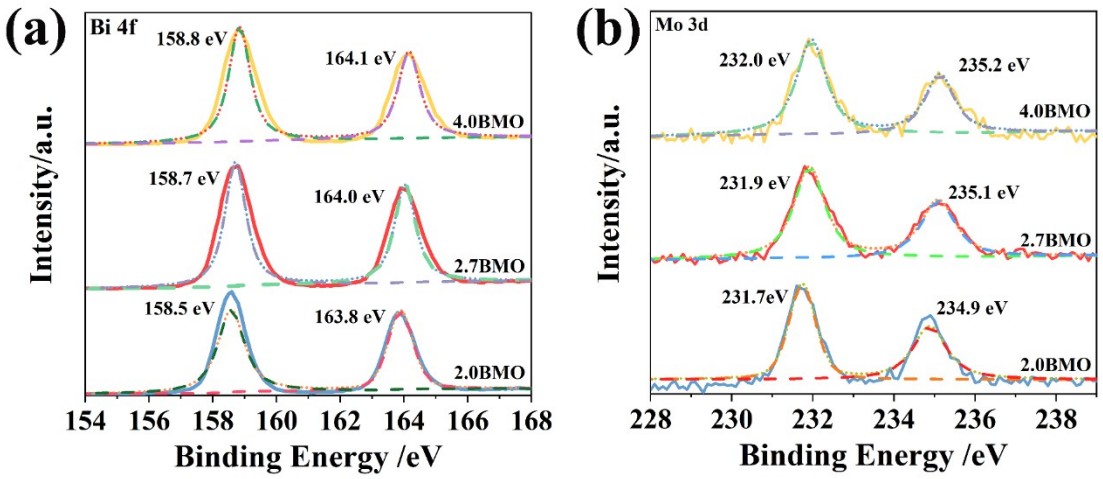

Fig. S6. Bi 4f (a) and Mo 3d (b) XPS of 2.0BMO, 4.0BMO, and 2.7BMO.

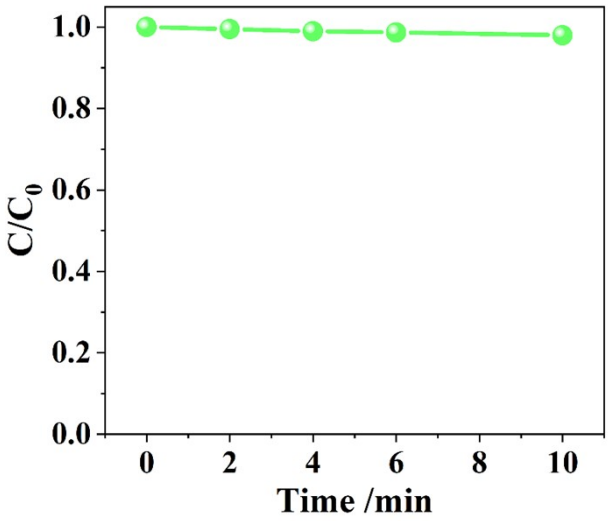

Fig. S7. The self-degradation activities of TC under visible-light without the photocatalysts.

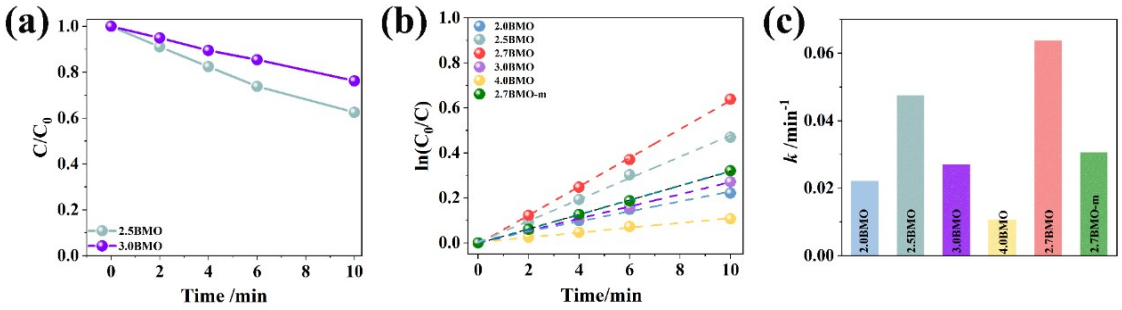

Fig. S8. (a) Photocatalytic activities of TC over 2.5BMO and 3.0BMO under visible-light irradiation, (b) pseudo-first-order decay curves of xBMO for TC degradation, and (c) *k* of xBMO for TC degradation.

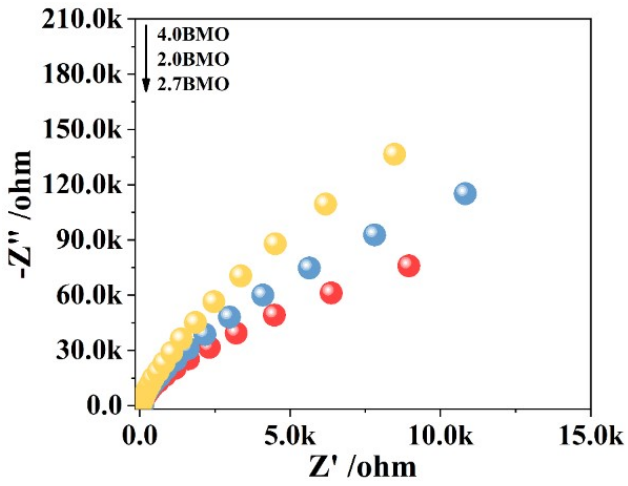

Fig. S9. Nyquist plots of 2.0BMO, 4.0BMO, and 2.7BMO.

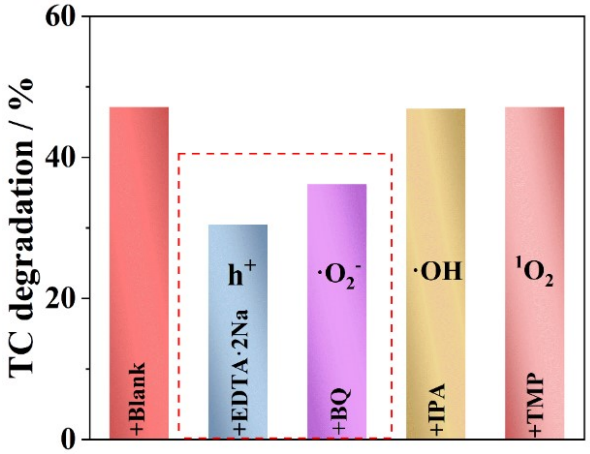

Fig. S10. Effects of radical scavengers on photocatalytic degradation of TC over 2.7BMO under visible-light irradiation.

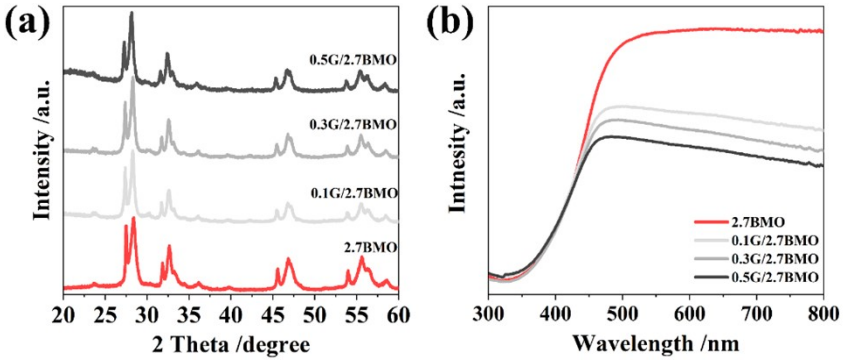

Fig. S11. XRD patterns (a) and UV-Vis DRS (b) of 2.7BMO and yG/2.7BMO.

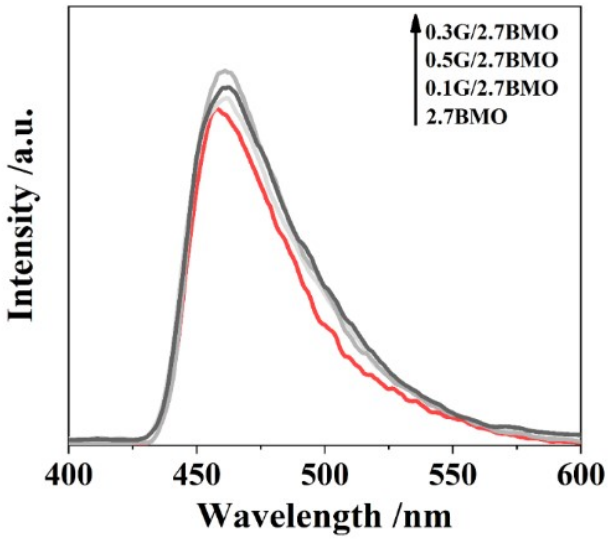

Fig. S12. FS related to the amount of formed hydroxyl radicals of 2.7BMO and yG/2.7BMO.

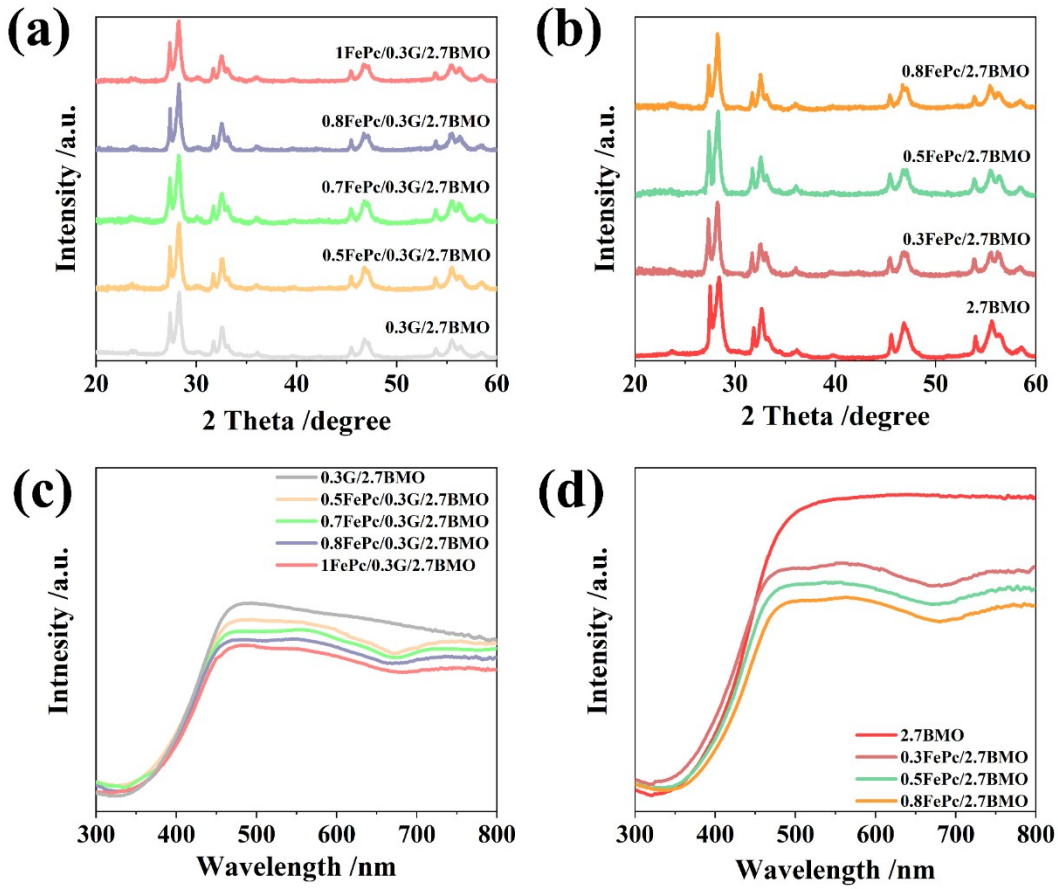

Fig. S13. XRD patterns (a, b) and UV-Vis DRS (c, d) of different samples.

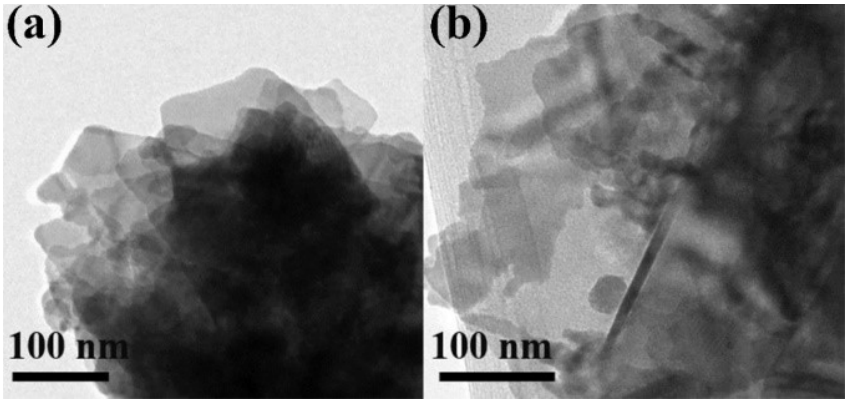

Fig. S14. TEM images of 0.8FePc/2.7BMO (a) and 0.8FePc/0.3G/2.7BMO (b).

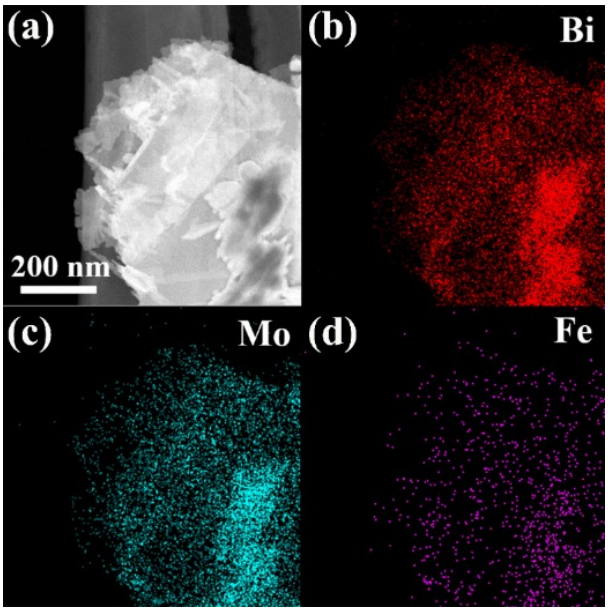

Fig. S15. High-angle annular dark-field scanning TEM images (a), the corresponding EDX mapping images of Bi (b), Mo (c), and Fe (d) of 0.8FePc/0.3G/2.7BMO.

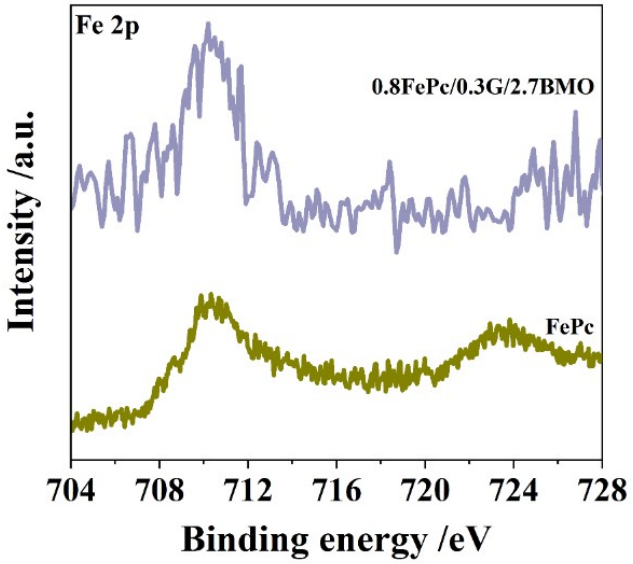

Fig. S16. Fe 2p XPS of FePc and 0.8FePc/0.3G/2.7BMO.

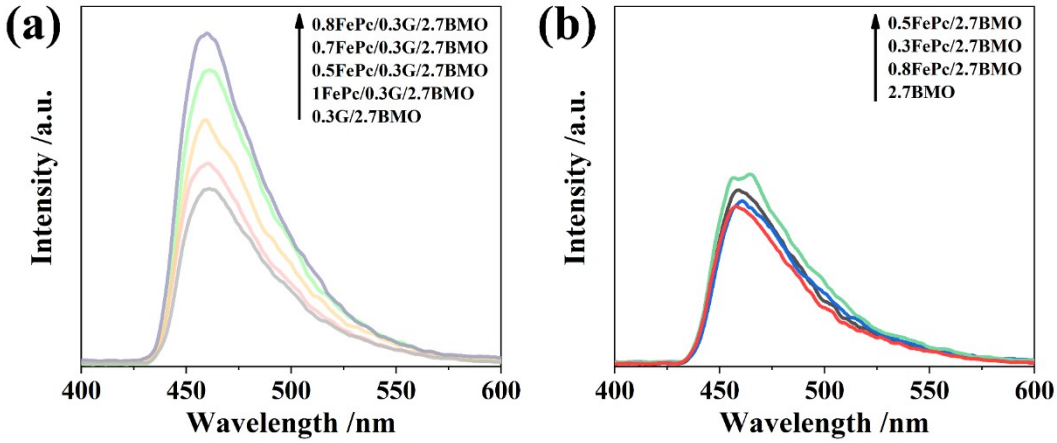

Fig. S17. FS related to the amount of formed hydroxyl radicals of 0.3G/2.7BMO and zFePc/0.3G/2.7BMO (a), and 2.7BMO and zFePc/2.7BMO (b).

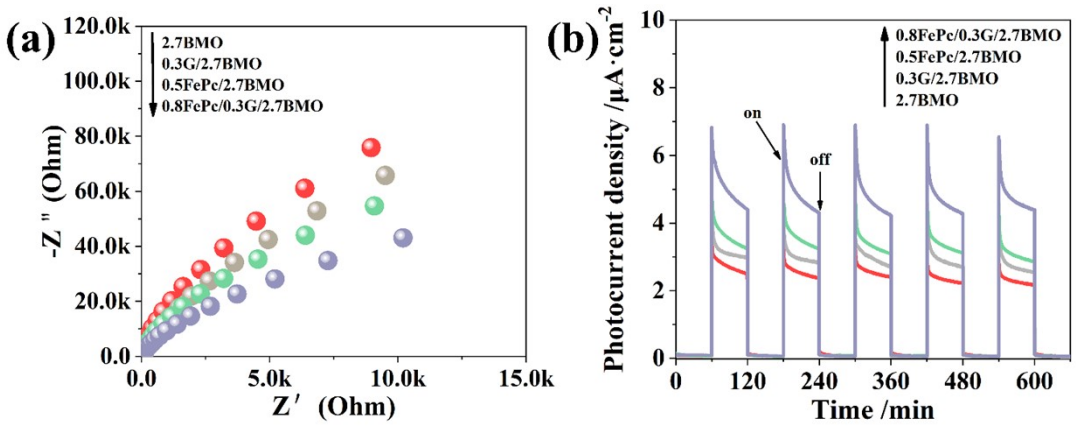

Fig. S18. Nyquist plots (a) and transient photocurrent densities (b) of different samples.

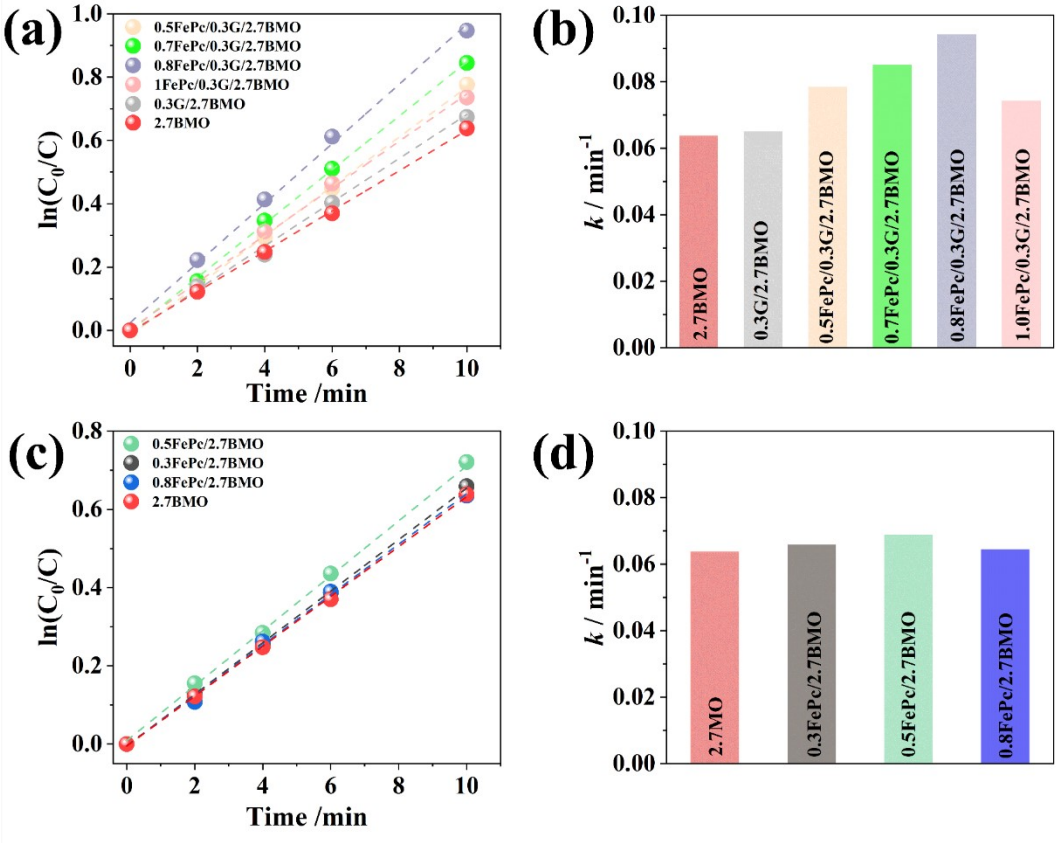

Fig. S19. Pseudo-first-order decay curves (a, c) and *k* (b, d) of different samples.

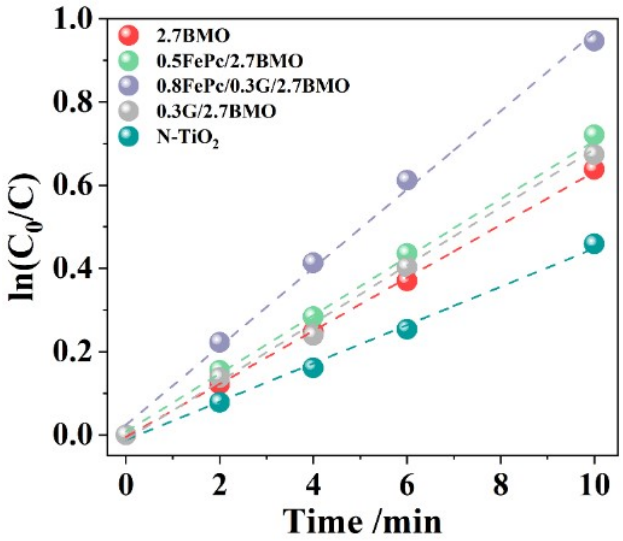

Fig. S20. Pseudo-first-order decay curves of different samples under visible-light irradiation.

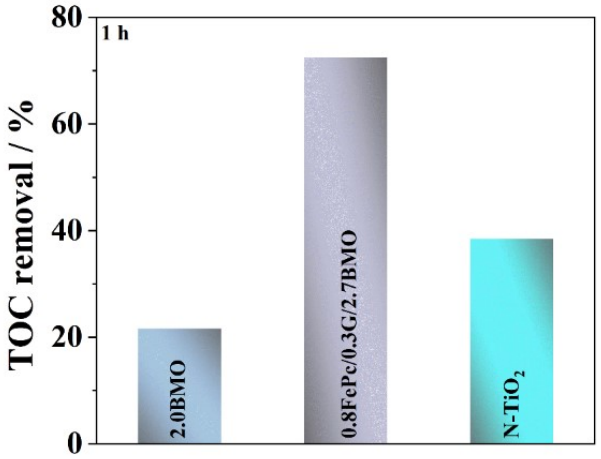

Fig. S21. TOC removal of different samples under visible-light irradiation.

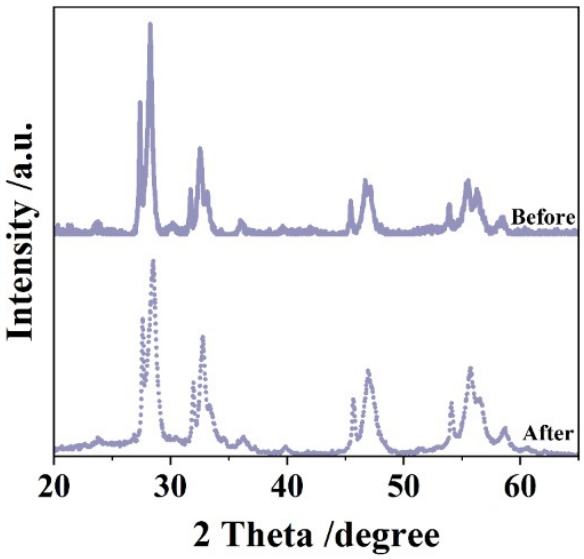

Fig. S22. XRD patterns of 0.8FePc/0.3G/2.7BMO before and after photocatalytic TC degradation.

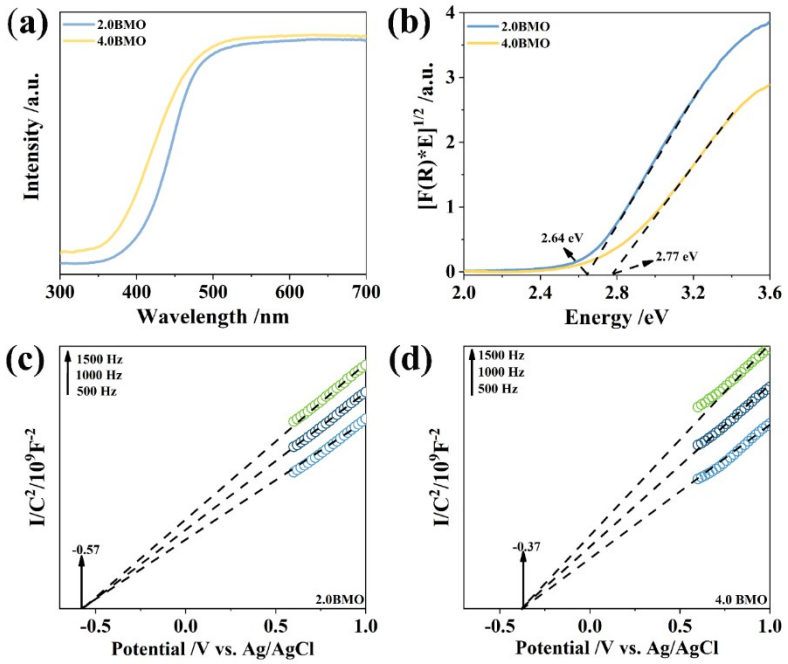

Fig. S23. UV-Vis DRS (a) and K-M function versus photon energy (b) of 2.0BMO and 4.0BMO, Mott-Schottky plots of 2.0BMO (c), and 4.0BMO (d).

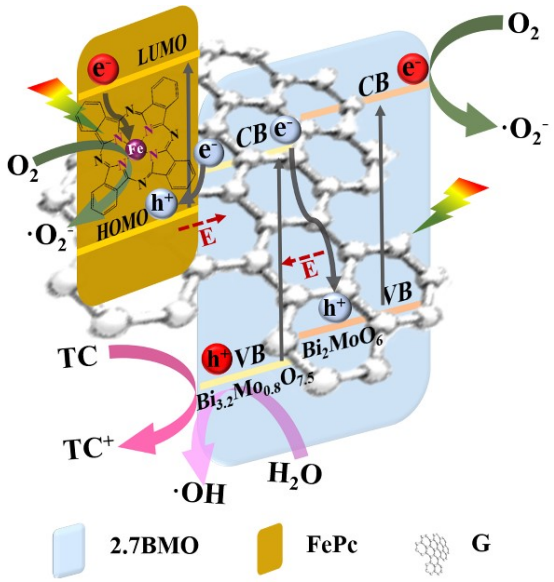

Fig. S24. Another possible mechanism of photogenerated charges transfer/separation and the subsequently induced reactions on dual S-scheme 0.8FePc/0.3G/2.7BMO heterojunction.

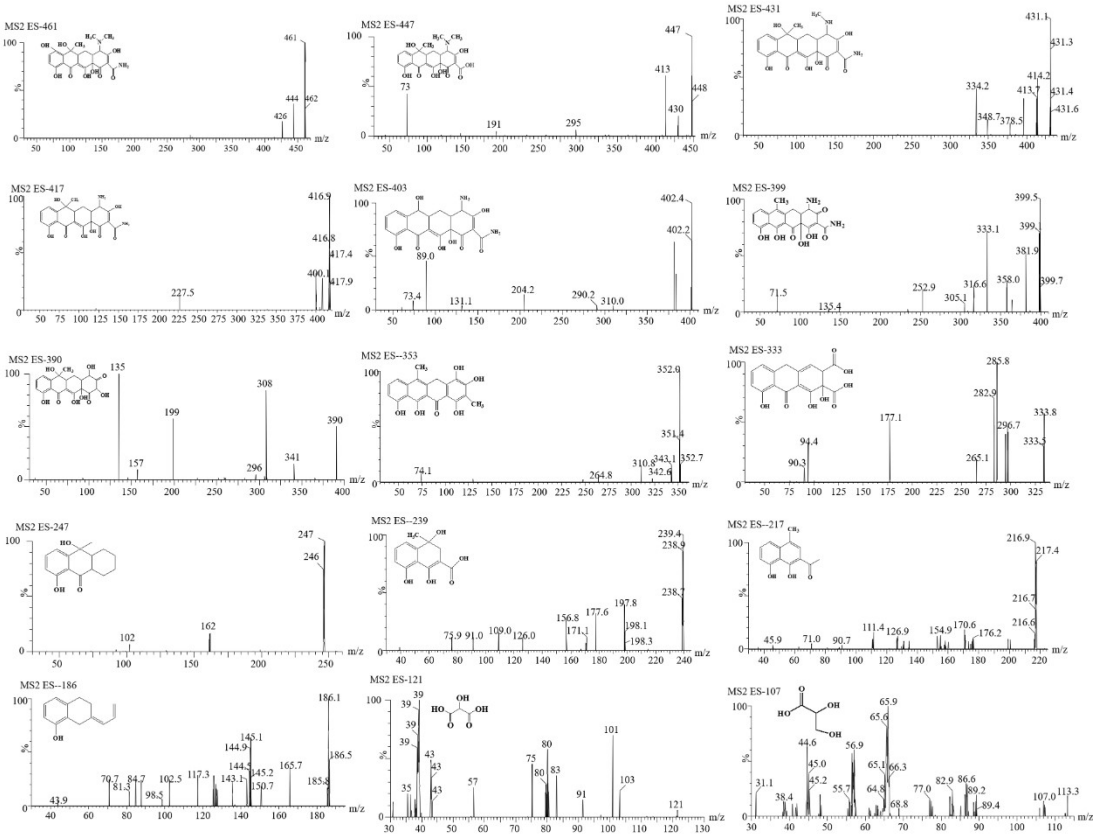

Fig. S25. Extracted ion chromatogram **(**EIC) analysis of the intermediate products after photocatalytic TC degradation over 0.8FePc/0.3G/2.7BMO.